



Synthesis, Characterization and Mechanical Properties Enhancement of Graphene Oxide doped Poly (vinylidene fluoride) nano-membranes



CrossMark

M. K. Abdelmaksoud^{1,2}, Alaa Mohamed^{3,4}, Abderrahman Sayed,^{1,2*} S. A. Khairy¹

¹Physics Department, Faculty of Science, Cairo University, Giza, Egypt.

²Faculty of Nanotechnology for postgraduate studies, Cairo University, El-Sheikh Zayed 12588, Egypt.

³Department of Mechatronics, Canadian International College, Fifth Settlement, New Cairo, Egypt

⁴Institute of Functional Interfaces (IFG), Karlsruhe Institute of Technology (KIT), Hermann-von-Helmholtz-Platz 1, 76344 Eggenstein-Leopoldshafen, Germany

THE graphene oxide is successfully prepared by applying the modified Hummers method. Poly (vinylidene fluoride)–Graphene oxide nanofiber membranes are synthesized with electrospinning technique. The prepared nanofiber membranes are carefully examined to ensure their single phase and compound structure formation as well as to measure their equivalent membrane diameter distributions. The samples were characterized with several tools like XRD, FTIR, and FESEM to prove their purity and to discover the samples microstructure. The corresponding cyclic mechanical properties are tested with the Dynamic Mechanical Analyzer (static mode).

Keywords: Graphene Oxide; Poly (vinylidene fluoride) (PVDF); Mechanical properties; Nano-membranes.

Introduction

While there are many different techniques to yield nanofibers (NFs) including drawing, phase separation, template synthesis, and self-assembly, an extra unique artificial technique, electrospinning, has attracted much attention lately [1]. Electrospinning is a clean and low-cost method to yield polymeric fibers with variable sections from micro-to- nanoscale and provide unbroken NFs with the essential properties in a simple way [2]. The main aim of electrospinning is to yield homogeneous NFs with small diameters [3]. NFs have great specific morphology, physicochemical properties, great flexibility for physicochemical surface functionalization, small pore size, and small diameters [4-6]. Furthermore, NFs have several properties that make them attractive for numerous applications such as, regenerative

medicine, biotechnology, and filtration membranes [2]. The mechanical properties of NFs are dependent on many parameters, such as the polymer material selection, polymeric solution composition, varying processing parameters, or applying post electrospinning treatments [5]. Furthermore, the optimization of electrospinning processing parameters is essential to enhance the mechanical properties of the composite NFs [7]. Moreover, the mechanical modulus and strength of the NFs depend on bonding between NFs, fiber orientation, and the slip of one fiber over another [5]. Because of a very small dimension of NFs, the mechanical properties tests of composite NFs is remaining a challenge for the current test instruments, which is the reason of rare scientific articles of NFs mechanical tests [8, 9]. It is expected that the mechanical properties of NFs

*Corresponding author: abdelrahmansayed@gstd.sci.cu.edu.eg

DOI :10.21608/ejphysics.2020.46172.1055

Received : 13/10/2020; accepted : 14/10/2020

©2021 National Information and Documentaion Center (NIDOC)

will increase by doping them with graphene oxide (GO). Specifically, GO improves NFs strength and provides them with outstanding properties, such as high modulus to weight ratio and high strength [5]. Moreover, Poly(vinylidene fluoride) (PVDF) demonstrates extraordinary mechanical, chemical, and thermal stability properties. It possesses five crystalline polymorphs phases, according to the preparation method [10]. Only three of these phases are polar and reveal ferroelectric and piezoelectric properties [11]. The most frequently explored phases, as a result of their outstanding properties and extensive applications, are called α , β , and γ [12]. In this study, we applied the electrospinning technique in producing Poly(vinylidene fluoride) membranes with and without graphene oxide. The aim is to enhance the mechanical properties of the nano-membrane, such that the membrane will sustain higher aqua pressures.

Experimental

Materials

Graphite powder with a particle size of 150 mesh 90% min, from Nice chemicals, Sulfuric acid (98%) from S D Fine., Potassium permanganate (98%) from El Goumhouria Co., Hydrochloric acid (37%) from Honeywell, Acetone (2-propanone, 99.5%) from Diachem, N, N-dimethyl formamide (99%) from Alfa Aesar, Hydrogen peroxide (30%) from PioChem, Poly(vinylidene fluoride) (PVDF) pellets (Mw = 275000) from Sigma Aldrich.

Preparation of graphene oxide (GO)

GO is synthesized by the modified Hummers method where an excessive oxidation technique of graphite is performed by adding KMnO_4 and H_2SO_4 . First, 2 g of graphite powder was stirred in 98% H_2SO_4 (45 mL) for one hour. Then a 6 g of KMnO_4 was gradually added to the above solution while keeping the temperature at less than 20 °C through an ice bath. After the temperature is stabilized, the solution is kept under stirring at room temperature for another hour and half. Then, the ice bath is used again and the solution is diluted through the addition of 90 mL of distilled water, while maintaining a vigorous stirring. Moreover, 10 mL of H_2O_2 solution (30%) and 150 mL of distilled water were added. The produced graphene oxide (GO) is then washed with a 5% HCl aqueous solution followed by distilled-water wash during several centrifuge cycles until the solution is neutralized [13]. GO was then dried below 60 °C to avoid the reduction into graphene oxide (RGO) (Fig. 1.) [14].

Preparation of PVDF-GO nanofibers

PVDF-GO nanofiber membranes are synthesized with electrospinning technique. A solution of 20 wt.% of PVDF pellets and 0.3 wt.% of GO is mixed with a DMF/acetone (v/v 3/2) solvent and sonicated for 15 min. Next, the prepared solution is stirred at a temperature lower than 60 °C for 2hr to obtain a homogeneous solution. The solution was then filled into a 5mL syringe with a 22 gauge needle. The syringe is positioned vertically for a minute and the air is completely removed. The flow rate is controlled by NE-300 (New Era Pump System Inc.) and the voltage supply is a 73030N (Genvolt General High Voltage Ind. Ltd.). The membranes are formed by applying a flow rate of 1 mL/h, a voltage of 23.5 kV, and a TCD (tip to collector distance) of 15 cm. As the last step, the membrane was left to dry at room temperature (Fig. 2.).

Results and Discussion

Characterization

The tensile test of nanofibers was measured by Dynamic mechanical analyzer DMA 25, Metravib (ACOEM Group). Scanning electron microscopy was carried out using FE SEM-Quanta FEG-250, Thermo Fisher Scientific. Whereas, the X-ray powder diffraction calculations were performed on D8 Discover, Bruker, where $\text{Cu-K}\alpha$ radiation was used with a wavelength of 1.540 Å. Fourier-transformed infrared spectroscopy spectra were recorded on Nicolet 6700 FT-IR with smart ITR, Thermo Scientific.

Materials characterization

XRD analysis was used to characterize the phase purity of the synthesized GO, the XRD pattern of the as-purchased graphite and GO is shown in Fig. 3. The diffraction peak of graphite powder is found around 26° and for GO a sharp peak at 10° was correlated to the (001) inter-layer structure of GO sheets [15]. The disappearance of the graphite peak and the appearance of the GO peak shows that the graphite powder is completely oxidized to GO by exfoliation and chemical oxidation [16].

Figure 4. Shows that PVDF NFs are generally in the α crystalline phase as shown by the existence of the two intensive peaks at 18.4° and 20.0° and the presence of the two weak peaks at 26.6° and 35.9°. On the other hand, the PVDF nanofibers with 0.3 wt.% GO show the existence of a very strong diffraction peak at 20.6° and the presence of a weak peak at 36.3° and can be considered as β crystalline phase of PVDF [17].

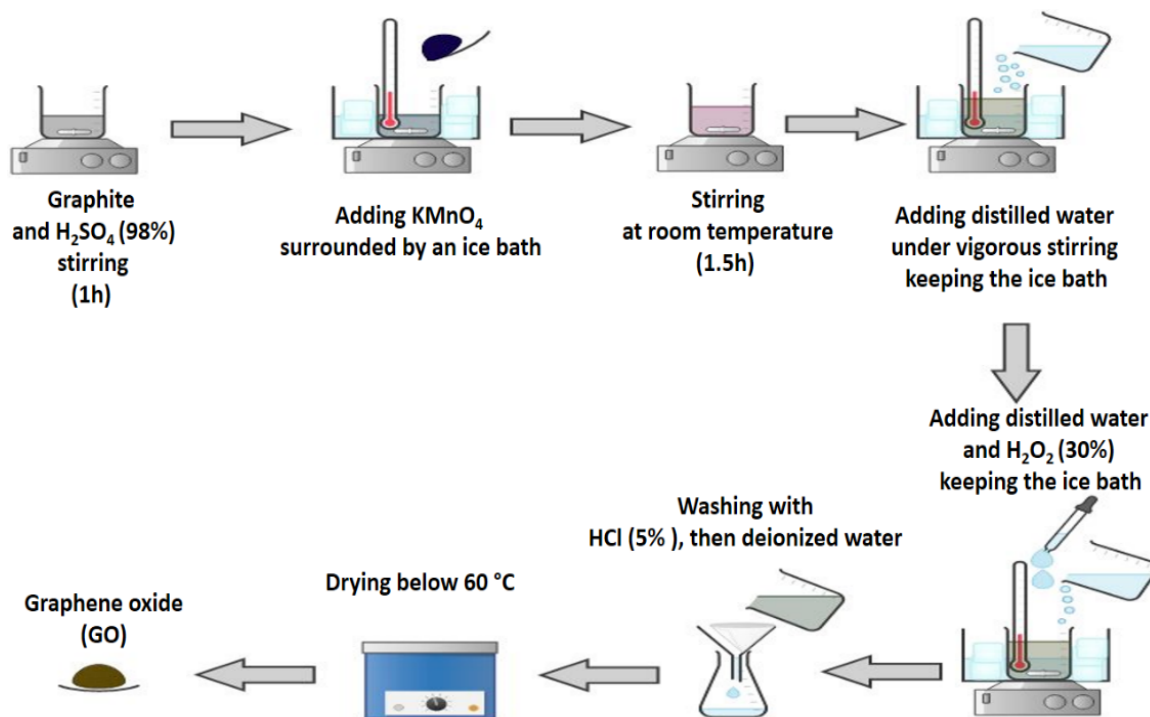


Fig. 1. Preparation of graphene oxide (GO).

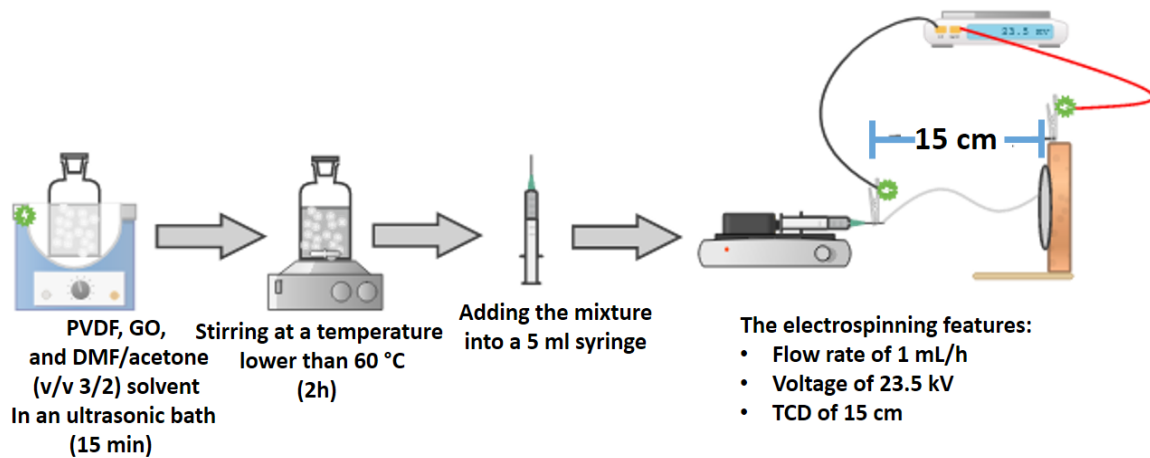


Fig. 2. Preparation of PVDF-GO nanofibers.

Fig. 5. FTIR of prepared GO.

The recorded FTIR spectrum of GO displays bands at 1050, 1250, and 1403 cm^{-1} that correspond to C–O, C–O–C, and C–OH bonds, respectively. The peak at 1620 cm^{-1} is a resonance peak of the C–C stretching as well as the absorbed OH groups in the GO [13]. However, the band in the range 1700–1600 cm^{-1} is due primarily to the C=O

stretching vibration [18]. Furthermore, the band around 2350 cm^{-1} indicates chemisorbed CO₂ [19]. Normally, the presence of OH and CO functional groups is anticipated as the measurements are performed in-air. [20]. Fig. 5. Shows the specific, slightly shifted, peak that characterize the prepared GO.

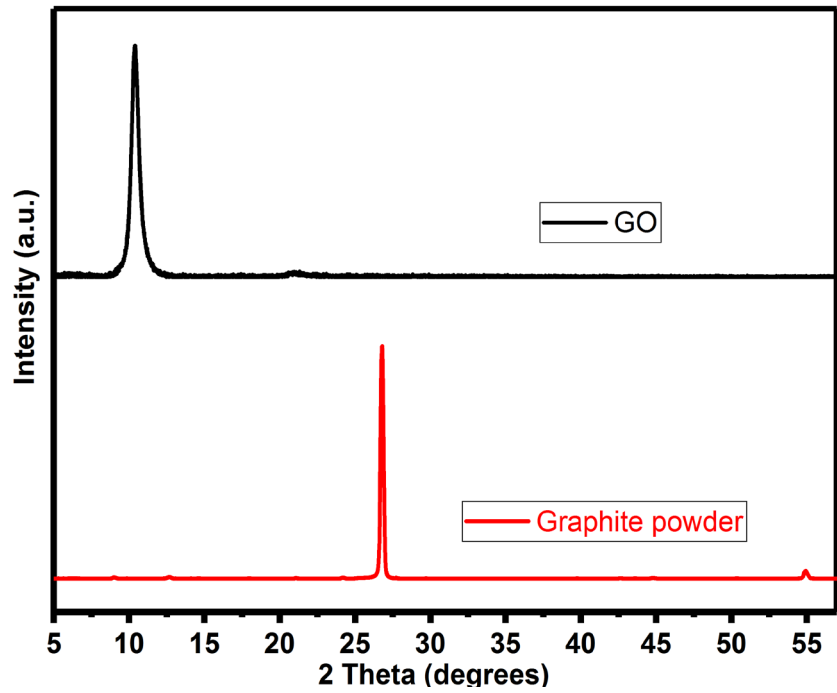


Fig. 3. XRD of graphite powder and GO.

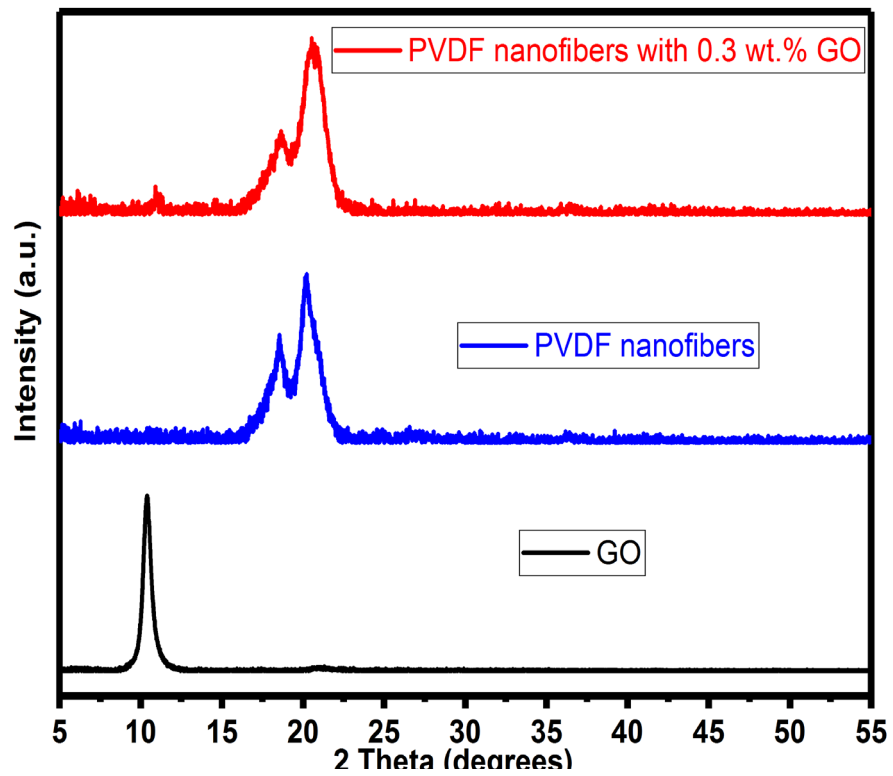


Fig. 4. XRD of GO, PVDF NFs, PVDF NFs with 0.3 wt.% GO.

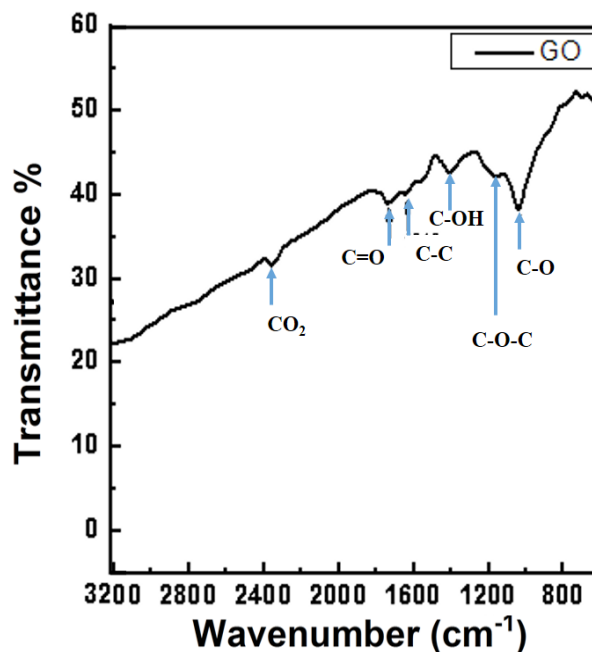


Fig. 5. FTIR of GO, PVDF NFs, PVDF NFs with 0.3 wt.% GO.

The FTIR spectra of the PVDF nanofibers are shown in Fig. 5. Several absorption bands at 764, 976, and 978 cm^{-1} were ascribed to the α -phase of the PVDF [21]. The most dominating peaks for the α -phase at 614 and 762 cm^{-1} are for the bending and wagging vibration of the CF_2 group and the rocking of the main PVDF chain, respectively [14]. After doping with GO, the peaks assigned to the β -phase became significantly stronger and sharper, while the peaks corresponding to the α -phase became indistinctive [21]. Therefore, GO leads to the transformation from α - to β -crystalline phase [14]. The use of GO as a nanofiller provided effective dipole polarization in the PVDF matrix and facilitated the nucleation of β -phase crystals due to the enhanced dipole-dipole forces. Moreover, Graphene possesses carbon atoms with a zigzag structure, which matches the zigzag structure of the β -phase. The attachment of PVDF chains to the GO sheets leads to the interaction between CF_2 in PVDF and the $\text{C}=\text{O}$ and COOH groups of the GO (hydrophilic interaction). Besides, the GO layers acts as a nucleating agent for the β -phase and as a hindering agent for the α -phase [21]. The nanofibers with 0.3 wt.% of GO particles, confirming a well-developed β -crystalline phase because of strong Van der Waals interactions between the highly electronegative fluorine on the PVDF chains

and the free electron pairs on the GO oxygen atoms. This probably forced the arrangement of the PVDF chains into a β -conformation when crystallizing on the GO surface [14].

The SEM micrographs in Fig. 6 illustrates the adhesion of GO flakes on the PVDF NFs surface. The micrographs demonstrate that the GO flakes are mixed with the NFs.

The NFs seem denser for the pure PVDF polymer (Fig. 7a). The two micrographs contain non-uniform fibers, but the degree of non-uniformity is greater for the PVDF-GO hybrid (Fig. 7b). The average diameters are calculated from the fiber histograms as 642 and 358 nm for the pure polymeric and hybrid NFs, respectively. The NF diameter and morphology depend on many polymeric solution parameters like viscosity, surface tension, electrical conductivity, and concentration. Moreover, they are also influenced by device parameters like high voltage value and tip-collector distance. Increasing net charge density and the surface tension coefficient favors the formation of smaller diameter NFs [22]. Where, net charge density = jet current x collecting time x concentration x solution density / mass of dry polymer. On the other hand, the polymeric jet becomes highly unstable at higher voltage, and thicker NFs are formed but with a

high standard deviation of the fiber diameter, which is a consistent description of our data [23]. Moreover, the hybrid fibers show several scattered beads. Typically, the solution viscosity, surface tension, and the net charge density of the electrospinning jet are the main factors of electrospun beads formation [22].

The sample dimensions for the dynamic mechanical analyzer (DMA) were 24.6 mm, 0.41 mm, 7.6 mm for PVDF NFs and 25.7 mm, 0.1 mm, 8 mm PVDF NFs with 0.3 wt.% GO. Normally, Young's modulus (E) is measured from the initial slope of the stress-strain curve. Specifically, it is the ratio of the stress (σ) to the corresponding strain (ϵ) in the initial linear part of the stress-strain curve [24, 25]. DMA device is utilized to attain the static cyclic stress-strain curves which demonstrate that the hybrid PVDF NF with 0.3 wt.% GO has a higher Young's Modulus of (5.07 ± 0.06) MPa compared to (1.89 ± 0.08) MPa for the pure PVDF NF polymer. The

loop area for the hybrid exceeds that of PVDF, as displayed in Fig. 8. Whereas, the loop ends earlier for the hybrid sample. Therefore, adding such a slight proportion of GO leads to increasing Young's modulus by more than 2.5 times. The hybrid sustains much higher stress which means that it becomes harder as a result of the GO accumulation.

Conclusion

The Poly (vinylidene fluoride)-Graphene Oxide membrane is successfully prepared. The average diameters for the pure polymeric and hybrid NFs are calculated as 642 and 358 nm, respectively. In agreement with previous research, GO doping leads to the transformation from α - to β -crystalline phase of PVDF. Adding a minute amount of GO leads to an augmentation of blended membranes Young's modulus by more than 2.5 times. This is an outstanding enhancement in the membrane mechanical properties.

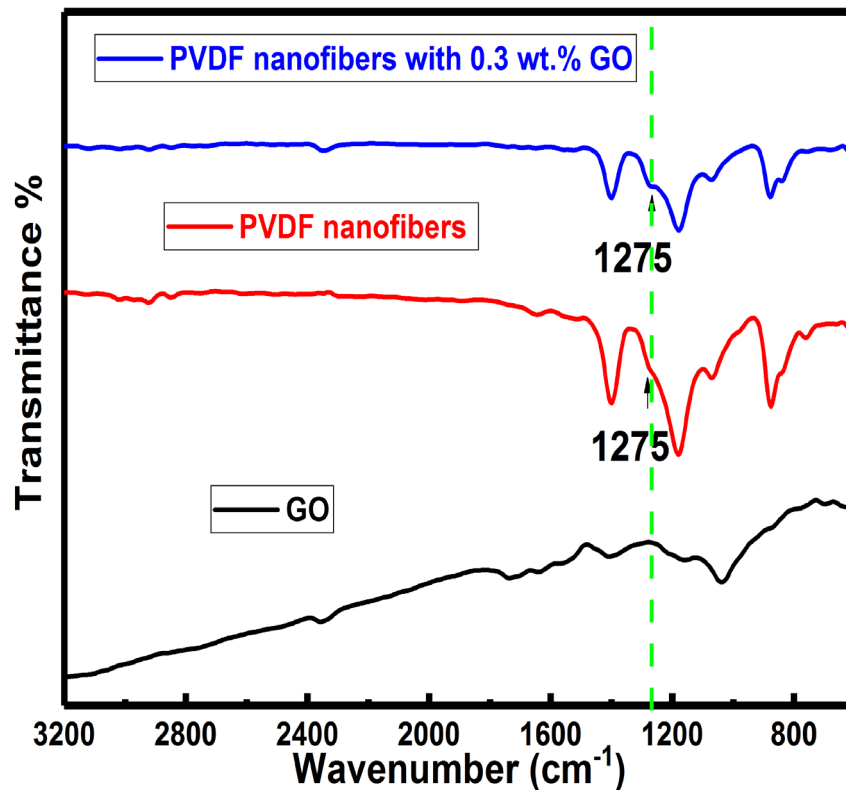


Fig. 6. FTIR of GO, PVDF NFs, PVDF NFs with 0.3 wt.% GO.

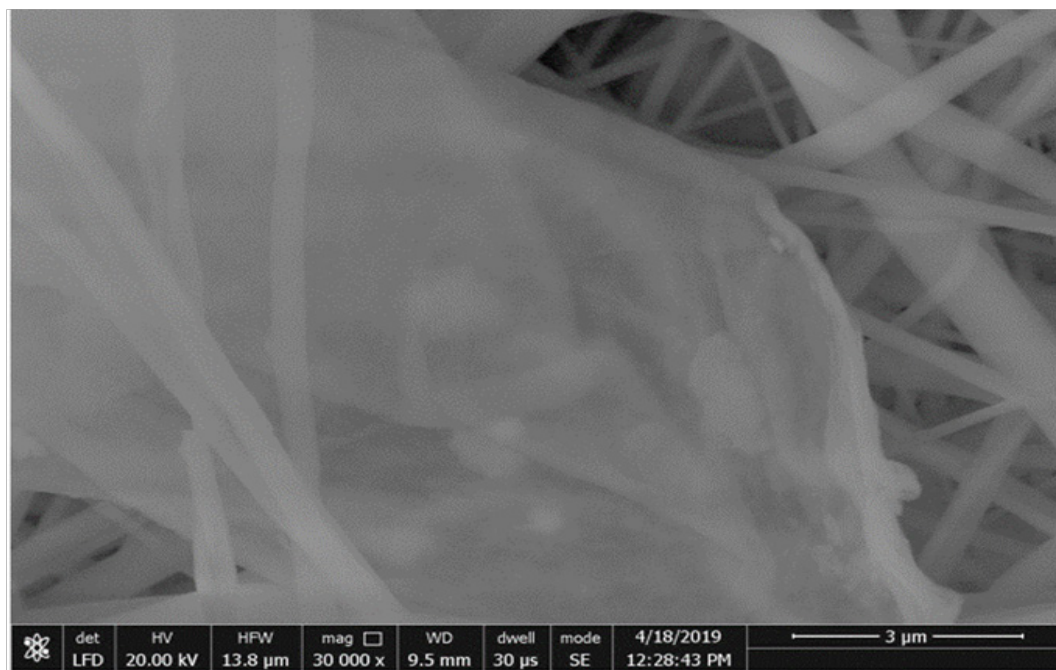


Fig. 7. FESEM of GO flakes on the PVDF NFs surface.

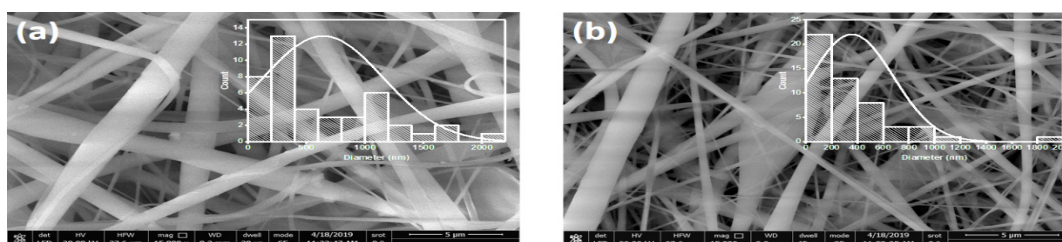


Fig. 8. FESEM of a) PVDF NFs, b) PVDF NFs with 0.3 wt.% GO, with the corresponding nanofibers diameter distribution as insets.

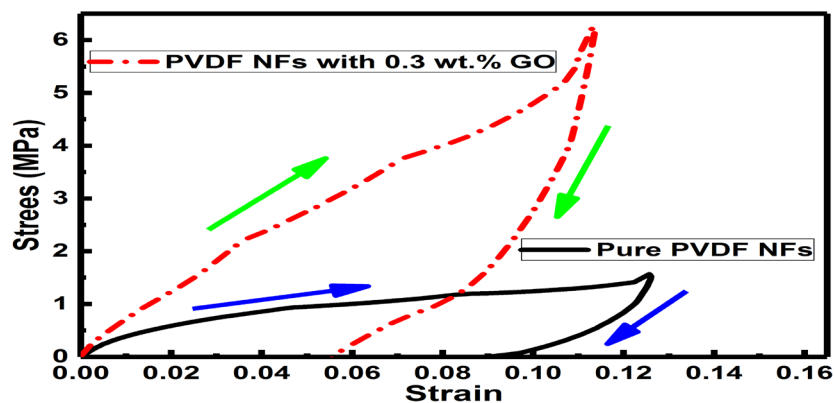


Fig. 9. Static cyclic stress-strain curves for pure and hybrid samples.

References

1. Schiffman, J. D. and Schauer, C. L., *Polymer Reviews*, **48** (2), 317-352 (2008).
2. Salama, A., Mohamed, A., Aboamera, N. M., Osman, T. and Khattab, A., *Advances in Polymer Technology*, **37** (7), 2446-2451 (2018).
3. Zhang, B., Kang, F., Tarascon, J.-M. and Kim, J.-K., *Progress in Materials Science*, **76**, 319-380 (2016).
4. Khalil, A., Aboamera, N. M., Nasser, W. S., Mahmoud, W. H. and Mohamed, G. G., *Separation and Purification Technology*, **224**, 509-514 (2019).
5. Aboamera, N. M., Mohamed, A., Salama, A., Osman, T. A. and Khattab, A., *Mechanics of Advanced Materials and Structures*, **26** (9), 765-769 (2017).
6. Mohamed, A., El-Sayed, R., Osman, T. A., Toprak, M. S., Muhammed, M. and Uheida, A., *Environ. Res.* **145**, 18-25 (2016).
7. Naraghi, M. and Chasiotis, I., in *Major Accomplishments in Composite Materials and Sandwich Structures* (Springer, 2009), pp. 757-778.
8. Mohamed, A., Yousef, S., Ali Abdrabelnaby, M., Osman, T. A., Hamawandi, B., Toprak, M. S., Muhammed, M. and Uheida, A., *Separation and Purification Technology*, **182**, 219-223 (2017).
9. Wang, S.-H., Wan, Y., Sun, B., Liu, L.-Z. and Xu, W., *Nanoscale Research Letters*, **9** (1), 1-7 (2014).
10. Salimi, A. and Yousefi, A. A., *Polymer Testing*, **22** (6), 699-704 (2003).
11. Castkova, K., Kastyl, J., Sobola, D., Petrus, J., Stastna, E., Riha, D. and Tofel, P., *Nanomaterials* **10** (6), 1221 (2020).
12. Ruan, L., Yao, X., Chang, Y., Zhou, L., Qin, G. and Zhang, X., *Polymers*, **10** (3), 228 (2018).
13. Krishnamoorthy, K., Veerapandian, M., Yun, K. and Kim, S. J., *Carbon*, **53**, 38-49 (2013).
14. Issa, A. A., Mariam Al Ali, S., Mrlík, M. and Luyt, A. S., *Journal of Polymer Research*, **23** (11) (2016).
15. Xu, Z., Wu, T., Shi, J., Teng, K., Wang, W., Ma, M., Li, J., Qian, X., Li, C. and Fan, J., *Journal of Membrane Science*, **520**, 281-293 (2016).
16. Paulchamy, B., Arthi, G. and Lignesh, B. D., *Journal of Nanomedicine & Nanotechnology*, **06** (01) (2015).
17. Cai, X., Lei, T., Sun, D. and Lin, L., *RSC Advances*, **7** (25), 15382-15389 (2017).
18. Coates, J., *Encyclopedia of Analytical Chemistry: Applications, Theory and Instrumentation* (2006).
19. Drouet, C., Alphonse, P. and Rousset, A., *Physical Chemistry Chemical Physics*, **3** (17), 3826-3830 (2001).
20. Xu, C., Shi, X., Ji, A., Shi, L., Zhou, C. and Cui, Y., *PLOS ONE* **10** (12), e0144842 (2015).
21. Abbasipour, M., Khajavi, R., Yousefi, A. A., Yazdanshenas, M. E. and Razaghian, F., *Journal of Materials Science: Materials in Electronics*, **28** (21), 15942-15952 (2017).
22. Fong, I. C. H., Reneker, D.H., *Polymer*, **40** 4585-4592 (1999).
23. Motamedi, A. S., Mirzadeh, H., Hajiesmaeilbaigi, F., Bagheri-Khoulenjani, S. and Shokrgozar, M., *Progress in Biomaterials*, **6** (3), 113-123 (2017).
24. Tsuchiya, T., Hirata, M. and Chiba, N., *Thin Solid Films*, **484** (1-2), 245-250 (2005).
25. Aravas, N. and Laspidou, C. S., *Biotechnol Bioeng*, **101** (1), 196-200 (2008).

تحضير وتوصيف وتحسين الخواص الميكانيكية لأغشية بولي (فلوريد فينيلدين) النانومترية المغطاة بأكسيد الجرافين

محمد خير الله عبد المقصود^{1,2,3}, علاء محمد³, عبدالرحمن سيد^{1,2}, شريف احمد خيرى¹

¹ قسم الفيزياء - كلية العلوم - جامعة القاهرة - الجيزة - مصر.

² كلية تكنولوجيا النانو للدراسات العليا - جامعة القاهرة - الشيخ زايد - مصر.

³ قسم الميكاترونكس - الكلية الكندية الدولية - التجمع الخامس - القاهرة الجديدة - مصر

⁴ معهد الاسطح الوظيفية- معهد كارلسروه للتكنولوجيا - ألمانيا

يتم تحضير أكسيد الجرافين بنجاح بتطبيق طريقة هامرز المعدلة. يتم تصنيع أغشية البولي (فلوريد فينيلدين) المطعمة بأكسيد الجرافين بتقنية الغزل الكهربائي. يتم فحص أغشية الألياف النانومترية المحضرة بعناية للتأكد من تكوين المركبات دون أي اختلاط مع مواد أخرى (الطور الأحادي) وكذلك لقياس التوزيعات الاحصائية لقطر الألياف النانومترية. تم توصيف العينات بعدة أدوات مثل جهاز حيود الأشعة السينية (XRD) وجهاز خيوليات فورير لامتناس الأشعة تحت الحمراء (FTIR) و جهاز المجهر الإلكتروني الماسح (FESEM) لإثبات نقائها ودراسة شكلها تحت المجهر الإلكتروني. يتم اختبار الخواص الميكانيكية الاستاتيكية الدورية باستخدام جهاز التحليل الميكانيكي الديناميكي (DMA).